Therapeutics, Targets, and Chemical Biology

Cancer Research

α2-Macroglobulin Inhibits the Malignant Properties of Astrocytoma Cells by Impeding β-Catenin Signaling

Inge Lindner[1], Nasr Y.A. Hemdan[2,6,7], Martin Buchold[1], Klaus Huse[8], Marina Bigl[1], Ilka Oerlecke[1], Albert Ricken[3], Frank Gaunitz[4], Ulrich Sack[2,6], Andreas Naumann[6], Margrit Hollborn[5], Dietmar Thal[9], Rolf Gebhardt[1], and Gerd Birkenmeier[1]

Abstract

Targets that could improve the treatment of brain tumors remain important to define. This study of a transformation-associated isoform of α2-macroglobulin (A2M*) and its interaction with the low-density lipoprotein receptor-related protein-1 (LRP1) suggests a new mechanism for abrogating the malignant potential of astrocytoma cells. LRP1 bound A2M* found to be associated with an inhibition of tumor cell proliferation, migration, invasion, spheroid formation, and anchorage-independent growth. Transcriptional studies implicated effects on the Wnt/β-catenin signaling pathway. Notably, LRP1 antibodies could phenocopy the effects of A2M*. Our findings suggest a pathway of tumor suppression in astrocytoma that might be tractable to therapeutic exploitation. *Cancer Res; 70(1); 277–87. ©2010 AACR.*

Introduction

The role of α2-macroglobulin (A2M) in tumorigenesis is closely related to its receptor, the low-density lipoprotein receptor–related protein 1 (LRP1). The possible mechanisms by which LRP1 regulates tumor cell behavior are related to its function as an endocytic receptor for proteases and protease inhibitors and its ability to regulate expression and catabolism of proteins, cell signaling, and the activity of adjacent membrane receptors (1). Nascent A2M is known to inactivate proteases accompanying tumor cell invasion such as plasmin, urokinase-type plasminogen activator, and metalloproteases (MMP; refs. 2, 3). Binding to proteases or small amines *in vitro* induces a conformational change in the A2M molecule that triggers its interaction with LRP1 (4) and creates distinct binding sites for transforming growth factor (TGF)-β1 (5) and other growth-regulating ligands (6) that can be rapidly cleared by LRP1 (7–9).

Glial tumors are among the most malignant intrinsic brain tumors, characterized by excessive proliferation, angiogenesis, and infiltration (10). Only few reports illuminate the possible function of LRP1 in these aggressive tumors, and results obtained are rather controversial (11). In addition, the effect of the proteinase inhibitor A2M on glial tumors has thus far not been addressed.

The present study aimed at exploring the impact of A2M* on various malignancy-associated properties of 1321N1 astrocytoma cells. Results imply that A2M* inhibits proliferation, migration, invasion, spheroid formation, and anchorage-independent growth of astrocytoma cells possibly through interfering with the Wnt/β-catenin signaling. The canonical pathway is known to play a pivotal role in cell malignant transformation (12). Wnt ligands form a ternary complex with frizzled receptor (FZD) and with the coreceptors LRP5/6, and this complex ultimately prevents the degradation of β-catenin. The latter accumulates in the nucleus and complexes with the transcription factors T-cell factor/lymphoid enhancer factor (TCF/LEF) to activate the transcription of target genes encoding various events of tumorigenesis.

We show that A2M* at nanomolar concentrations induced the expression of LRP1, FZD, E-cadherin, and N-cadherin and inhibited Wnt ligand expression. This provides evidence for the LRP1-mediated suppressive potency of A2M* and offers a promising approach for tumor treatment.

Materials and Methods

Reagents. Anti-human LRP1 monoclonal antibody (mAb; clone II2C7 and II4/8), rabbit polyclonal anti-LRP1 antibody (Ab), native A2M, methylamine-transformed A2M*, and FITC-A2M* were purchased from BioMac; the WST-1 proliferation kit was from Roche; cellulose nitrate membranes were from Whatman Schleicher & Schuell; DMEM and RPMI medium, FCS, and Cy3-labeled goat anti-mouse Ab were from Invitrogen; Growth Factor Reduced Matrigel Matrix and polycarbonate mesh, mouse anti-human E-cadherin,

Authors' Affiliations: [1]Institute of Biochemistry, [2]Clinical Immunology and Transfusion Medicine, [3]Institute of Anatomy, [4]Clinic for Neurosurgery, and [5]Department of Ophthalmology, University of Leipzig; and [6]Fraunhofer Institute for Cell Therapy and Immunology, Leipzig, Germany; [7]Department of Zoology, Faculty of Science, University of Alexandria, Alexandria, Egypt; [8]Leibniz Institute for Age Research-Fritz Lipmann Institute, Jena, Germany; and [9]Institute of Pathology-Laboratory of Neuropathology, University of Ulm, Ulm, Germany

Corresponding Author: Gerd Birkenmeier, Institute of Biochemistry, University of Leipzig, Johannisallee 30, 04103 Leipzig, Germany. Phone: 49-341-9722132; Fax: 49-341-9722109; E-mail: Gerd.Birkenmeier@medizin.uni-leipzig.de.

doi: 10.1158/0008-5472.CAN-09-1462

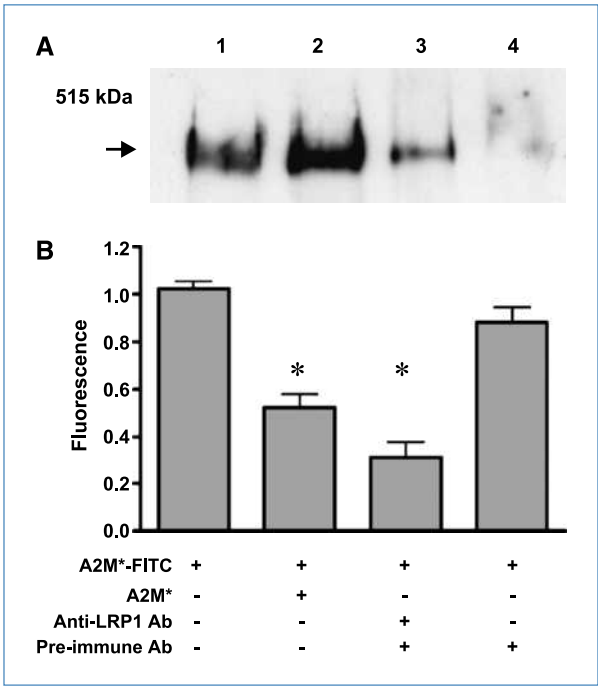

Figure 1. Immunodetection of the LRP1 protein in 1321N1 astrocytoma cells and analysis of cellular uptake of FITC-labeled A2M*. *A,* cellular extracts of human astrocytoma, fibroblasts, LNCaP, and DU-145 prostate cancer cells (50 μg each, *lanes 1–4*, respectively) were subjected to SDS-PAGE and Western blotting. *B,* uptake of A2M*-FITC by astrocytoma, and competition by A2M* (2 μmol/L) and anti-LRP1 Ab (2 μmol/L). Preimmune Ab (2 μmol/L) was used as a control. Samples were measured in triplicates ($n = 6$; *, significance at $P < 0.05$).

N-cadherin, and β-catenin were from BD Biosciences; hematoxylin was from Merck; trypan blue was from Seromed; rabbit anti-human β-actin Ab was from Abcam; horseradish peroxidase (HRP)–labeled goat anti-mouse Ab and real detection system peroxidase/3,3′-diaminobenzidine rabbit/mouse kit were from Dako; protease inhibitor cocktail was from Sigma-Aldrich; and the chemiluminescence detection kit was from Boehringer. Plasmid *pCMV-GLUC* was obtained from Prolume Nanolight, Inc.; the TCF Reporter Plasmid kit was from Millipore; TransIT-LT1 was from Mirus Corporation; and the *Gaussia* luciferase transfection kit and coelenterazine were from PJK. A2M (clone α1-IIE7) and prostate-specific antigen (PSA; clone 1B7) mAbs were used as described previously (13, 14).

Cell lines. Human astrocytoma 3121N1 cells (European Collection of Animal Cell Cultures; 86030102), LNCaP (DSMZ; ACC 256), PC-3 (CRL-1435; American Type Culture Collection), and DU-145 (DSMZ; ACC 261) were used for this study.

Cell culture. Human astrocytoma 1321N1cells were cultured in DMEM, 10% FCS (DMEM-FCS), 100 units of penicillin, and 100 μg streptomycin/mL at 37°C/5% CO_2 in a humidified atmosphere. Cell monolayers were dissociated using 0.04% trypsin/0.03% EDTA in 50 mmol/L PBS (pH 7.4). Cellular protein extracts of tumor cells were prepared using an extraction buffer [25 mmol/L Tris, 2 mmol/L EDTA, 10% glycerol, 1% Triton X-100, 2 mmol/L DTT, and 1 mmol/L phenylmethylsulfonyl fluoride (pH 7.0)] containing 0.3% protease inhibitor cocktail. Protein content was determined (15) and human fibroblast cultures were set up (16) as previously described.

Endocytosis of FITC-labeled A2M. Astrocytoma cell cultures (10^5/2 mL DMEM-FCS/well) were set up and FITC-labeled A2M* (0.1 μmol/L) was added to cavities containing 2 μmol/L A2M*, 2 μmol/L polyclonal anti-LRP1 Ab, or rabbit preimmune immunoglobulin (2 μmol/L) and incubated for 30 min to estimate binding/uptake of labeled A2M*. Plates were chilled on ice, washed twice (each with 2 mL PBS), and supernatants were discarded. Cells were removed by trypsination and incubated with extraction buffer in the absence of protease inhibitors. Samples were disintegrated by sonication (3 × 15 s) and centrifugation at 13,000 rpm for 15 min at 4°C. Supernatants were analyzed using Perkin-Elmer LS50B.

Immunochemistry. According to standard protocols, immunochemical staining of astrocytoma 1321N1 cells was done using the primary anti-human Abs directed against

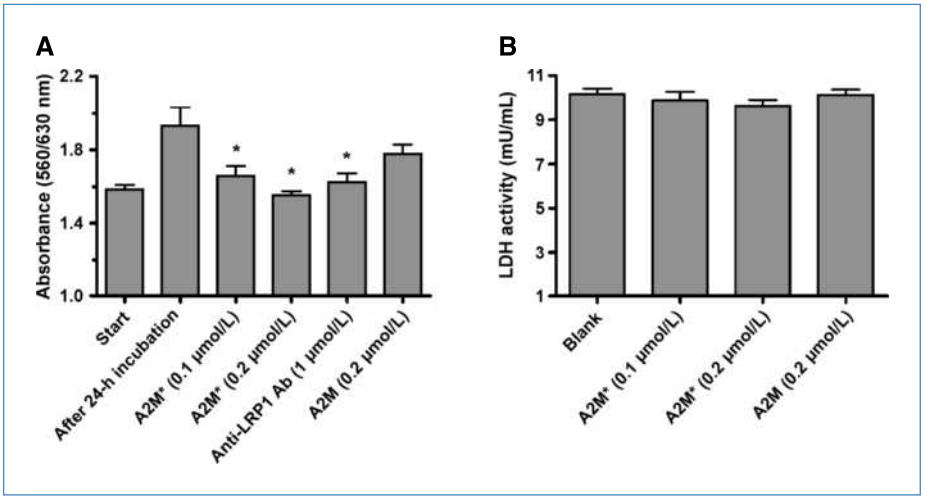

Figure 2. A2M* reduces proliferation/vitality but does not affect LDH release of 1321N1 astrocytoma cells. *A,* astrocytoma (5×10^5 cells/mL; *Start*) were cultured in complete medium for 24 h in the absence or presence of A2M*, A2M, or anti-LRP1 Ab. Cell vitality was assessed by the WST-1 assay. *Columns,* mean of six independent experiments; *bars,* SD. *B,* LDH activity (mU/mL) was measured in the supernatant upon incubation of tumor cells with A2M* or native A2M. *Columns,* mean of three replicates ($n = 6$; *, significance at $P < 0.05$); *bars,* SD.

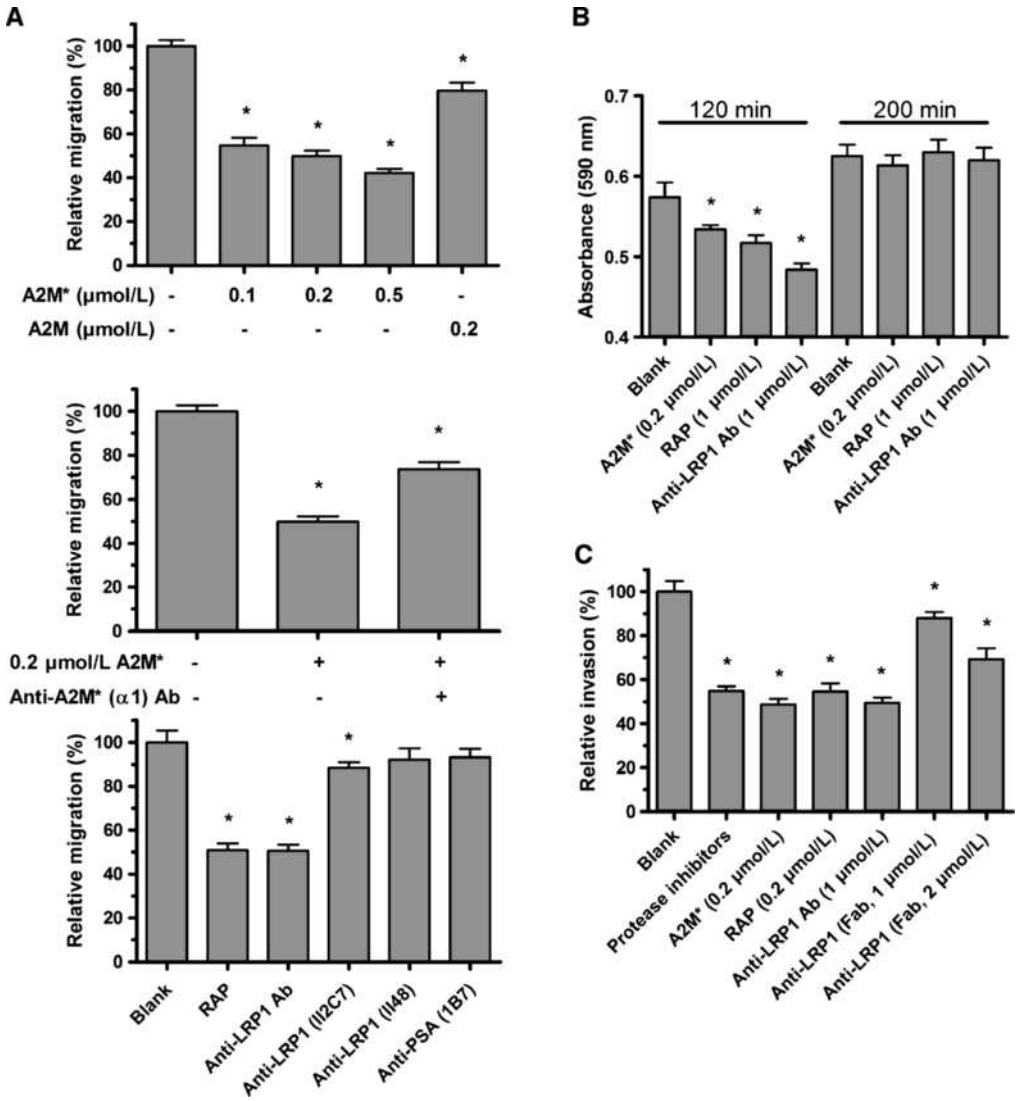

Figure 3. A2M* and LRP1 ligands inhibit migration, adhesion, and invasion of 1321N1 cells. *A,* dependence of migration of tumor cells on the concentration of A2M and A2M* (*top*), anti-A2M* mAb (clone α1-IIE7; 0.2 μmol/L) directed against LRP1-binding domain (*middle*), and RAP (0.2 μmol/L) polyclonal anti-LRP1 Ab (1 μmol/L) and various mAbs (0.2 μmol/L) directed against the 515-kDa (II2C7) and 85-kDa (II4/8) receptor subunit compared with an irrelevant anti-PSA mAb (*bottom*) compared with untreated cells (*Blank*). *B,* the effect of A2M* and LRP1 ligands on adhesion of 1321N1 cells at gelatin-coated 96-well plates measured at 120 and 200 min. *Columns,* mean of triplicates ($n = 6$; *, significance at $P < 0.05$); *bars,* SD. *C,* invasion was analyzed by coating the porous inserts with 25 μL Matrigel before seeding. Cell migration was analyzed in the absence or presence of a protease inhibitor cocktail (5 μL/mL), A2M*, RAP, anti-LRP1 Ab, and various concentrations of anti-LRP1 Ab-Fab fragments. *Columns,* mean ($n = 6$; *, significance at $P < 0.05$); *bars,* SD.

E-cadherin, N-cadherin, LRP1, β-catenin, and β-actin. Immunofluorescence detection was accomplished with Cy3-labeled goat anti-mouse Ab. Three-micrometer paraffin-embedded sections of spheroids were stained with mouse anti-LRP1 mAb (clone II2C7) in combination with a secondary biotinylated Ab and HRP-labeled streptavidin. Stained cells were evaluated with a confocal laser scanning microscope (LSM510 META, Carl Zeiss).

Immunoblotting. Following cell lysis, 20 to 100 μg of cell lysate proteins were loaded to 4% to 20% SDS-PAGE and then blotted to membranes. The primary Abs used were rabbit anti-LRP1 (1 μg/mL) and anti–β-actin Ab (0.5 μg/mL), anti–β-catenin, anti–E-cadherin, and anti–N-cadherin mAb (10 μg/mL each). Detection was accomplished with HRP-labeled goat anti-mouse (1:1,000) or anti-rabbit (1:2,000) Ab. Bands were visualized by chemiluminescence detection.

Proliferation/vitality. Astrocytoma cells were cultured as described above, putative receptor ligands were added, and cell proliferation was analyzed using the WST-1 assay (17).

Cell viability test. The effect of A2M* on viability of astrocytoma cells was inspected by trypan blue exclusion (18).

Lactate dehydrogenase release. Lactate dehydrogenase (LDH) activity was assayed in the supernatant of astrocytoma cells cultured for 24 h (17).

Migration and invasion assay. Cell movement was evaluated in Boyden chambers using 24-well culture plates equipped with 8-μm pore polycarbonate mesh; the bottom well was filled with 800 μL DMEM-FCS. For invasion analysis, the membranes of inserts were coated with 25 μL Growth Factor Reduced Matrigel Matrix. Cells (4×10^4 in 100 μL DMEM, 0.5% FCS) were seeded in the upper compartment to adhere overnight. Test substances were added and incubation was continued for 6 h (migration) or 42 h (invasion). Cells were removed and the membranes were fixed with Karnowski solution and stained with hematoxylin.

Anchorage-independent growth. Six-well plates were coated with 1.5 mL of a base layer of 0.6% basal agar in 2× DMEM-FCS. Cells (8×10^5/well) were added in a mixture of 0.4% agar and 2× DMEM/20% FCS. Test substances were initially mixed into the upper agar layer. Cultures were evolved for 14 d and replenished daily with 100 μL DMEM-FCS. Finally, the plates were stained with 0.5 mL of 0.005% crystal violet and colonies of >20 cells were counted.

Adhesion assay. Well plates were coated with 0.1% gelatin solution before adding 10^4 cells/100 μL DMEM-FCS in the absence or presence of A2M*, the receptor-associated protein (RAP), or anti-LRP1 Ab. After certain time lapses, nonadherent cells were washed away and the remaining cells were fixed with 4% paraformaldehyde solution, stained with crystal violet (1%), washed, and destained with acetic acid (33%) followed by reading the absorbance at 590 nm against the blank.

Tumor spheroid cultures. Astrocytoma cells (5×10^6) were transferred into 10 mL DMEM-FCS containing test substances in 50-mL plastic tubes and rolled at 5 rpm at

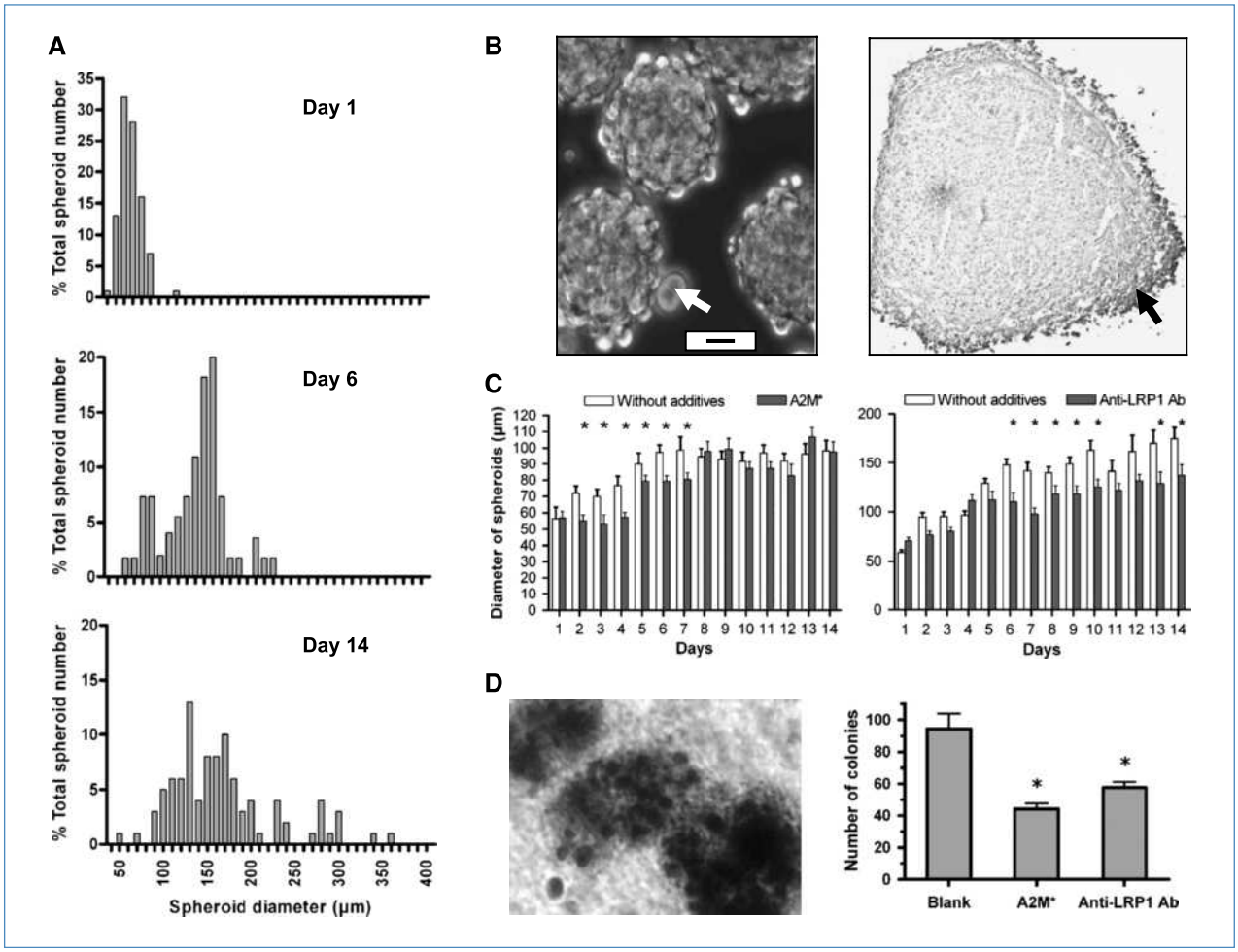

Figure 4. Exposure to A2M* or anti-LRP1 Ab inhibits formation of tumor spheroids and cell colonies. *A* to *C,* spheroid formation in the absence of A2M* and anti-LRP1. *A,* size distribution throughout 2 wk; *B,* light microscopy of a growing spheroid; *white arrow,* shedding of cells (*bar,* 5 μm) and immunostaining of LRP1 antigen in a 1-mm tumor spheroid; *black arrow,* the positive staining at the margin. *C,* change in spheroid size over time in the presence of 0.2 μmol/L A2M* or 1 μmol/L anti-LRP1 Ab. *Columns,* mean ($n = 70$; *, significance at $P < 0.05$); *bars,* SD. *D,* representative view of cell colonies and inhibition of colony formation of 1321N1 cells in soft agar by A2M* and anti-LRP1 Ab. *Columns,* mean of colony counts ($n = 8$; *, significance at $P < 0.05$); *bars,* SD.

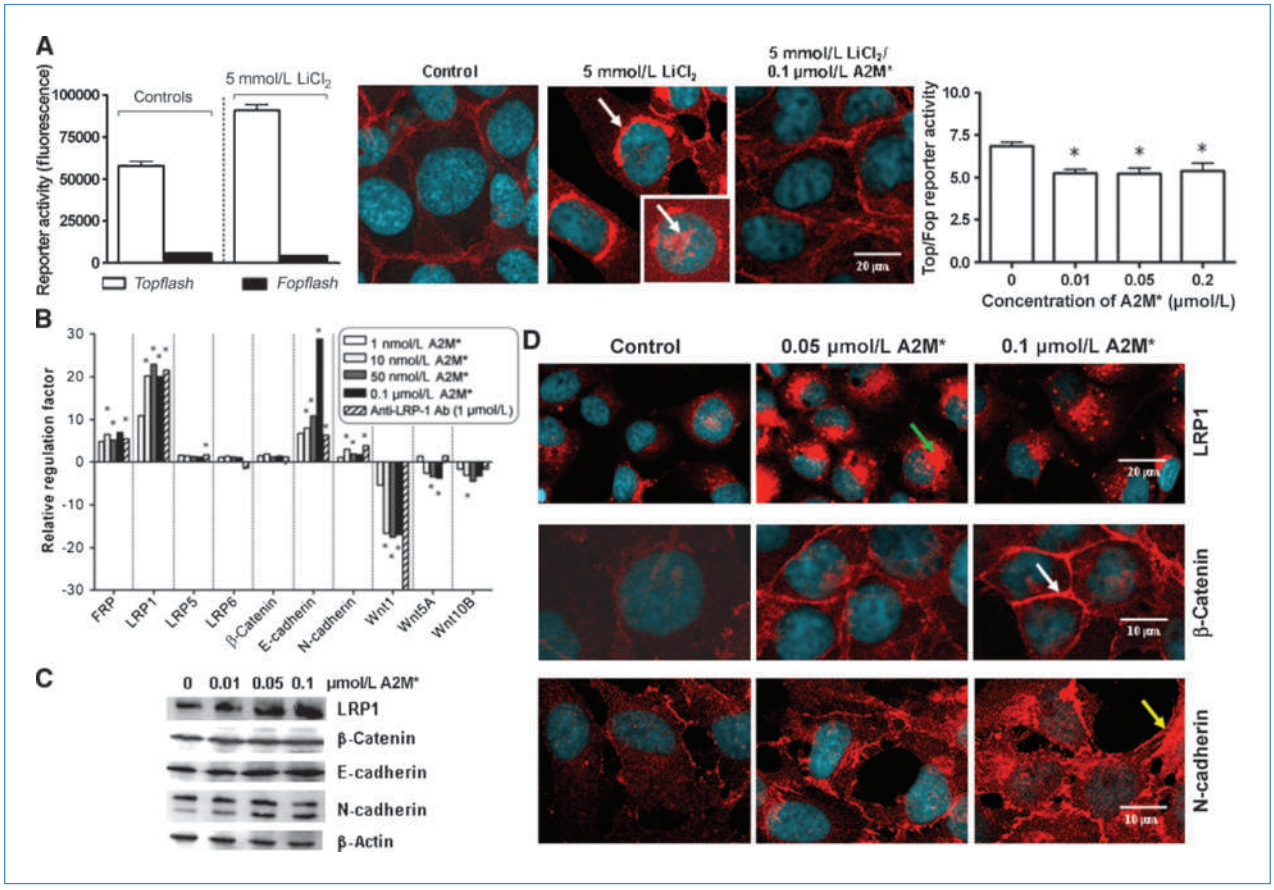

Figure 5. Modulation of the Wnt/β-catenin signaling pathway by A2M* in 1321N1 astrocytoma cells. *A,* activation of the constitutive Wnt/β-catenin pathway by $LiCl_2$ evaluated by *TopFlash/Fopflash* reporter assay. The activity of the *Fopflash*-reporter gene containing a mutated TCF-binding site was used as internal control (*left*). Immunochemical staining of β-catenin (*white arrow*) in untreated and cells treated with 5 mmol/L $LiCl_2$ and with 5 mmol/L $LiCl_2$/0.1 μmol/L A2M*; *inset,* nuclear localization of β-catenin (*middle*). *Right,* attenuation of the reporter gene activity by A2M*. *B,* relative expression of key genes of the Wnt/β-catenin signaling pathway following exposure to successive concentrations of A2M* or anti-LRP1 Ab (1 μmol/L). Plotted is the upregulation or downregulation factor relative to the untreated controls (GAPDH; assigned to 0). *, significance relative to controls. *C,* Western blot analysis of LRP1, β-catenin, E-cadherin and N-cadherin, and β-actin (*Control*) in 1321N1 cells treated with A2M* (0–0.1 μmol/L). *D,* immunostaining of LRP1 (*green arrow*), β-catenin (*white arrow,* relocated β-catenin in the plasma membrane), and N-cadherin (*yellow arrow*) in astrocytoma cells treated with 0.05 and 0.1 μmol/L A2M*.

37°C/5% CO_2 for 3 wk. Spheroid diameters (mean of two orthogonal diameters) were determined and the medium was changed daily.

Preparation of Fab fragments. Fab fragments of rabbit anti-LRP1 Ab (10 mg) were prepared using the Fab Preparation Kit from Pierce.

Relative gene expression. Isolation of total RNA of astrocytoma cells exposed to serial concentrations of A2M*, digestion of genomic DNA, reverse transcription, and purification of cDNA were done as previously described (19). For real-time PCR, the forward (f) and reverse (r) primer sequences used were as follows: (*a*) *GAPDH* (NM_002046.3), f: 5′-AGCCACATCGCTCAGACAC-3′ and r: 5′-GCCCAATACGACCAA ATC C-3′; (*b*) *LRP1* (NM_002332.2), f: 5′-GATGAGACACACGCCAACTG-3′and r: 5′-CGGCACTGGAACTCATCA-3′; (*c*) *LRP5* (NM_002335.2), f: 5′-GAACATCAAGCGAGCCAAG-3′and r: 5′-TGGCTCAGAGAGGTCAAAACA-3′; (*d*) *LRP6* (NM_002336.2), f: 5′-ATCCGAAAGGCACAAGAAGA-3′and r: 5′-GACTCGGAACTGAGCTCACAA-3′; (*e*) *FZD* (NM_001463.2), f: 5′-TCATGGGCTATGAAGATGAGG-3′ and r: 5′-TCATATCCCAGCGCTTAACTT T-3′; (*f*) *Wnt1* (NM_005430.2), f: 5′-CGCTGGAACTGTCCCACT-3′ and r: 5′-AACGCCGTTTCTCGACAG-3′; (*g*) *Wnt3A* (NM_033131.2), f: 5′-AACTGCACCACCGTCCAC-3′ and r: 5′-CCGACTCCCTGGTAGCTTT-3′; (*h*) *Wnt5A* (ENST00000264634.4), f: 5′-TAAGCCCAGGAGTTGCTTTG-3′ and r: 5′-CTGAACAGGGTTATTCATACCTAGC-3′); (*i*) *Wnt10B* (U81787.1), f: 5′-GCGAATCCACAACAACAGG-3′ and r: 5′-TCCAGCATGTCTTGAACTGG-3′; (*j*) *β-catenin* (X87838.1), f: 5′-GCTTTCAGTTGAGCTGACCA-3′ and r: 5′-AAGTCCAAGATCAGCAGTCTC A-3′; (*k*) *E-cadherin* (AB025105.1), f: 5′-CCCGGGACAACGTTTATTAC-3′ and r: 5′-GCTGGCTCAAGTCAAAGTCC-3′; and *N-cadherin* (M34064.1), f: 5′-GGTGGAGGAGAAGAAGACCAG-3′ and r: 5′-GGCATCAGGCTCCACAGT-3′. Reactions started by an initial activation step for 10 min at 95°C, and each following cycle

consisted of a denaturation step for 15 s at 94°C, annealing for 5 s at 60°C, and extension for 15 s at 72°C. *GAPDH* was chosen as a reference housekeeping gene as it showed amplification efficiency similar to those of other cytokine genes. REST software (20) was used to estimate gene expression relative to controls.

TCF reporter assay. The reporter gene *TOP-Gau* containing a secreted luciferase of *Gaussia princeps*, controlled by two sets of three copies of the TCF binding site (wild-type) and a thymidine kinase minimal promoter, was derived by combining the reporter gene *TOP-flash* (TCF Reporter Plasmid kit) with the luciferase gene. The luciferase coding

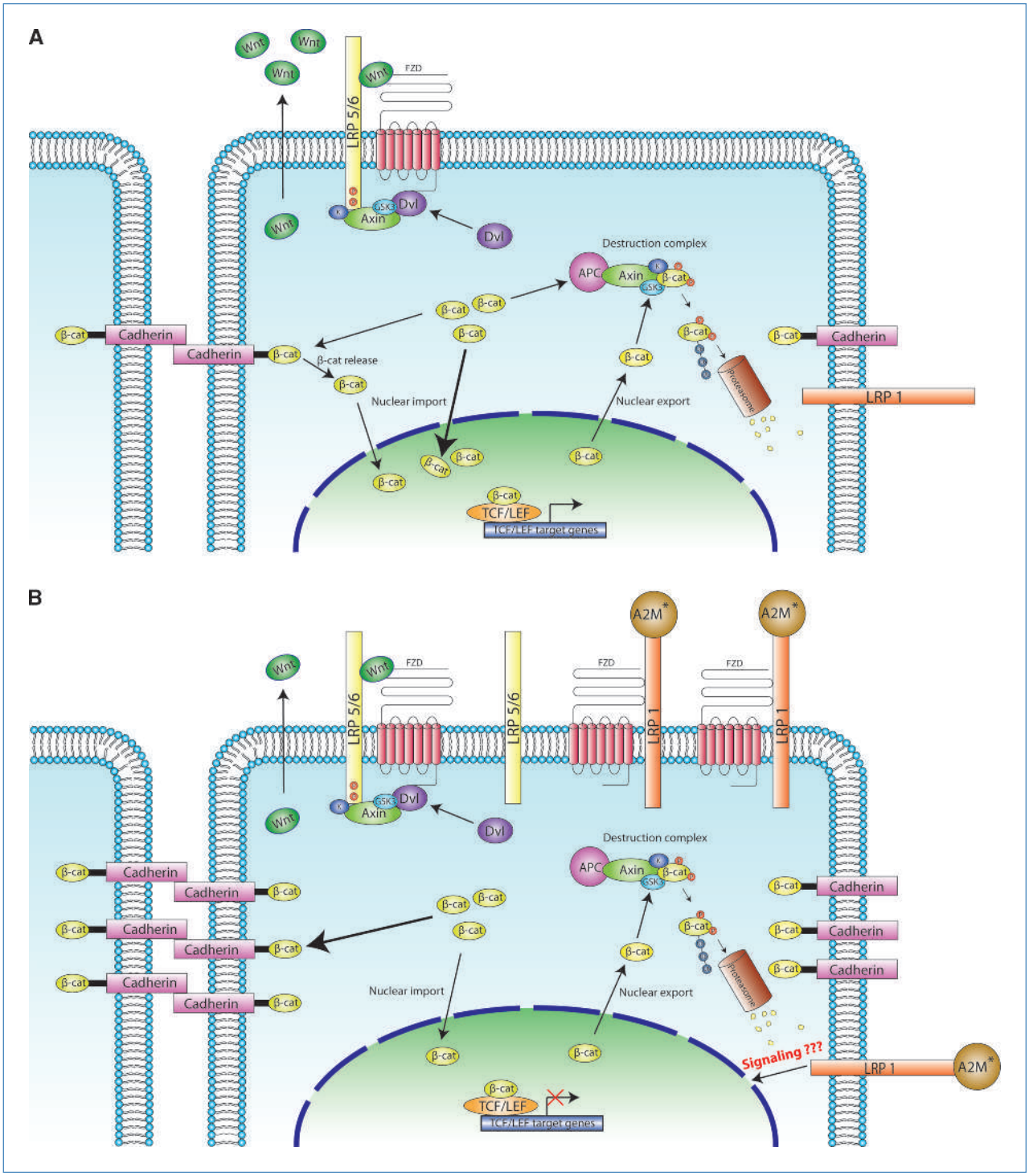

region was derived from the plasmid *pCMV-GLUC*. The mutated *FOP-Gau* reporter gene (with two full copies and one incomplete copy of the TCF binding site followed by three copies in the reverse orientation) was derived from *FOP-flash* and *pCMV-GLUC*.

Cells, seeded at 10^5 per 1 mL medium, were transfected with 1 μg DNA using TransIT-LT1, and then incubated with test substances for 36 h. *Gaussia* luciferase activity was assessed in 10 μL cell supernatants using 50 μL assay reagent on Orion-II microplate luminometer.

Statistical analysis. Statistics were done using Wilcoxon's rank-sum test, and PCR results were analyzed using pair-wise fixed reallocation randomization test incorporated in REST software; significance were considered at $P < 0.05$. Unless indicated otherwise, all data indicate means ± SD of three independent experiments.

Results

LRP1 is highly expressed in astrocytoma cells and mediates endocytosis of A2M*. LRP1 is apparently highly expressed in 1321N1 astrocytoma cells compared with two prostate cancer cell lines (LNCaP and DU-145) or fibroblasts (Fig. 1*A*). FITC-labeled A2M* was rapidly endocytosed by tumor cells; its uptake is diminished by adding nonlabeled A2M* or anti-LRP1 Ab (Fig. 1*B*), highlighting the ability of the polyclonal Ab to block the A2M* binding site of LRP1.

A2M* inhibits the growth factor–elicited cell proliferation. A2M* strongly inhibited proliferation of tumor cells under optimal growth-promoting conditions, whereas native A2M exerted only marginal inhibitory effects (Fig. 2*A*). To explore an alternative pathway other than neutralizing growth factors (21, 22), we blocked the cellular receptor with a polyclonal Ab that presumably does not mediate clearance of growth factors. As depicted in Fig. 2*A*, anti-LRP1 Ab exhibited a similar influence on cell proliferation compared with A2M*, a further clue for the LRP1 activation by A2M*. We assume that the polyclonal Ab fraction may contain mAb(s) that specifically reacted with the A2M* binding domain of LRP1 and can mimic the binding of A2M* to the receptor.

Inhibition of cell proliferation by A2M* was not due to cell toxicity as indicated by the unaltered LDH release (Fig. 2*B*). Moreover, the average cell vitality was 95 ± 3%, 93 ± 3.7%, and 96 ± 8% for control, 0.2 μmol/L A2M*, and 0.2 μmol/L A2M-treated cells, respectively.

A2M* inhibits migration, adhesion, and invasion of 1321N1 astrocytoma cells. The migration rate of 1321N1 cells was inversely correlated with the concentration of A2M*. As expected, cell migration was only slightly changed by native A2M (Fig. 3*A*). The specificity of A2M*-LRP1 interaction was confirmed by applying mAb (α1; clone α1-IIE7) known to react with the COOH-terminal receptor–binding domain of A2M* (13); its presence abrogated the inhibiting effect of A2M*, probably through blocking the binding of A2M* to LRP1. RAP, known to abolish binding of almost all ligands to LRP1 (23), diminished cell migration, similar to the polyclonal anti-LRP1 Ab. As controls, we used mAbs against α (II2C7) and β (II48) chains of LRP1 as well as an irrelevant Ab against PSA (1B7). All of these mAbs showed insignificant effects on cell migration.

Because A2M* and polyclonal anti-LRP1 Abs inhibited cell proliferation and migration, we hypothesize that inhibition may be due to LRP1-dependent interference with malignant cell adhesion factor(s). Results depicted in Fig. 3*B* showed that, compared with controls, the adhesion of tumor cells was significantly reduced after 120 minutes in the presence of 0.2 μmol/L A2M*, 1 μmol/L RAP, or 1 μmol/L polyclonal anti-LRP1. No difference between control and ligand-treated cells was observed following 200-min incubation. These data indicate that LRP1 might be involved in cell adhesion, and receptor ligands can diminish cell-matrix interaction.

Tumor cells invade extracellular matrix either through protease-dependent processes or amoeboid movement (24). Therefore, inhibiting extracellular proteases would eventually reduce the ability of cells to invade the matrix network. To prove this, a cell invasion assay was conducted to allow cells to migrate through Matrigel-coated 8-μm pore invasion chambers. In the presence of protease inhibitors, the invasion of tumor cells was reduced by ~50% relative to controls. Similar results were obtained by A2M*, polyclonal anti-LRP1 Ab, or RAP (Fig. 3*C*). The agonistic LRP1 mAb (clone II2C7) and the irrelevant anti-PSA mAb (1B7) failed to inhibit cell invasion. Because activated A2M* has lost its antiproteolytic activity, its effect on cell invasion may be possibly brought about

Figure 6. Inhibition of the Wnt/β-catenin (*β-cat*) pathway in astrocytoma cells following exposure to A2M*: a proposed mechanism. *A,* activation of the canonical Wnt pathway requires the binding of Wnt ligands to FZD together with the coreceptor low-density LRP5 and/or LRP6. The subsequent recruitment of Dishevelled (*Dvl*) and Axin initiates the phosphorylation of LRP5/6 and Dishevelled by various kinases (*K*) and ultimately the inactivation of glycogen synthase kinase-3β (*GSK3*). This circumvents phosphorylation of β-catenin that accumulates in the cytoplasm and translocates into the nucleus, where it binds to the TCF/LEF protein, forming a potent transcription regulatory complex. The latter activates the expression of target genes (*myc, cyclin D1, c-jun Axin, MMPs*) promoting tumor growth. In the absence of Wnt, β-catenin is phosphorylated by glycogen synthase kinase-3β–adenomatous polyposis coli tumor suppressor protein (*APC*)-Axin complex, initiating ubiquitination of β-catenin, and its subsequent degradation (13). Besides acting as a transcription regulator, β-catenin tightly associates to membrane-anchored cadherins and plays an essential role in cell-cell integrity and modulates various functions such as cell migration and adhesion. In this way, cadherins negatively regulate Wnt signaling by trapping β-catenin to the plasma membrane. It is not yet fully clear how the cellular pool of β-catenin—the membrane-bound β-catenin, the β-catenin of the destruction complex, or the nuclear β-catenin—is dynamically regulated. *B,* binding of A2M* or anti-LRP1 to LRP1 causes strong upregulation of LRP1, FZD, E-cadherin, and N-cadherin. LRP1 sequesters FZD and thereby disrupts the FZD-LRP5/LRP6 complex and ultimately represses the canonical Wnt pathway (48). Simultaneously, β-catenin relocates to the plasma membrane probably due to increased expression of cadherins, thereby increasing cell-cell integrity. Furthermore, inhibiting the expression of Wnt ligands by A2M* constitutes an additional way of negative regulation of Wnt/β-catenin signaling.

by direct activation of LRP1. This was corroborated by applying polyvalent and monovalent anti-LRP1 Ab obtained by papain digestion.

A2M* or anti-LRP1 Ab inhibits growth of spheroids and anchorage-independent growth of 1321N1 astrocytoma cells. Tumor spheroids provide a suitable three-dimensional *in vitro* model that may mimic the cellular environment of a poorly vascularized, hypoxic solid tumor (25). We monitored the growth of approximately 50 to 100 spheroids per group to study the size distribution over time. The initial aggregation of cells (over 3 days) showed cell clumps of 40 to 120 μm in diameter (Fig. 4*A*). The size of the spheroids increased progressively with time but size distribution became more heterogeneous due to shedding of tumor cells from surface and formation of subspheroids (Fig. 4*B, left*). Immunostaining of LRP1 (Fig. 4*B, right*) indicated its presence at the margin, which may constitute the proliferative zone of a spheroid. Results shown in Fig. 4*C* revealed that the diameter of the spheroids increased steadily up to day 6, then followed by a plateau phase till day 14. Compared with controls, A2M* (0.2 μmol/L) or anti-LRP1 Ab (1 μmol/L) inhibited the growth of tumor spheroids. A2M* was more potent at the initial phase of spheroid accretion comparable with anti-LRP1 Ab. This indicates the implication of LRP1 in cell-cell adherence and that ligation of the A2M* binding domain of LRP1 modulates this process.

Furthermore, we investigated the effect of A2M* and Abs on anchorage-independent growth, which is a good index of tumorigenicity. Astrocytoma cells were found to form colonies in the soft-agar assay (Fig. 4*D, left*) and A2M* (0.2 μmol/L) significantly inhibited colony formation by >50%. Compared with the control, polyclonal anti-LRP1 Ab elicited a similar effect (Fig. 4*D, right*).

A2M* mitigates the Wnt/β-catenin pathway in 1321N1 astrocytoma cells and increases expression of LRP1. Progression of human tumors is often associated with the induction of the canonical Wnt/β-catenin signaling. Using the *Topflash/Fopflash* assay, we found that the Wnt/β-catenin signaling is constitutively active in 1321N1 cells discernible at the high activity of the *Topflash* versus *Fopflash* signal (Fig. 5*A, left*); the latter was used as internal control. The functionality of the Wnt/β-catenin signaling cascade was shown by adding 5 mmol/L $LiCl_2$ that is known to inhibit glycogen synthase kinase-3β, leading to stabilization of β-catenin, which then accumulates around and translocates into the nucleus. This effect was notably abated in the presence of 0.1 μmol/L A2M*. β-Catenin is relocated to the plasma membrane (Fig. 5*A, middle*), implying inhibition of the canonical Wnt/β-catenin pathway by A2M* (Fig. 5*A, right*). This was additionally affirmed by evaluating the expression of various genes (Fig. 5*B*). Surprisingly, low doses of A2M* significantly upregulated FZD, LRP1, E-cadherin, and N-cadherin at the mRNA and protein levels, and slightly upregulated β-catenin levels (Fig. 5*C*); LRP5 and LRP6 mRNA remained unchanged. The expression of Wnt1, Wnt5A, and Wnt10B mRNA was downregulated (Fig. 5*B*), whereas Wnt3A mRNA was not detected. As expected, anti-LRP1 Ab exerted comparable effects.

As shown in Fig. 5*D*, A2M* increased the cellular level of LRP1 and induced the relocation of β-catenin to the plasma membrane. Apparently, in the presence of A2M*, the size of the cytosolic compartments and nuclei diminished in a dose-dependent fashion (*middle*).

Discussion

In the present study, we show that A2M* in conjunction with its receptor LRP1 inhibits migration, invasion, anchorage-independent growth, and formation of tumor spheroids of 1321N1 astrocytoma cells. Comparable to the native A2M, which does not bind to the receptor, the impact of A2M* implies that the activated protease inhibitor executes strong tumor-suppressive properties. Furthermore, we provide a novel evidence that A2M* mediates its effects through attenuating the Wnt/β-catenin signaling, which is upregulated in many tumors.

At present, the beneficial impact of A2M* on tumors and other diseases have been mainly discussed in terms of clearing growth factors, especially TGF-β1 that is known to strongly promote the malignancy of gliomas (9, 22, 26). However, our experiments with polyclonal Abs may argue against this assumption because growth factors cannot be cleared by them. This alludes that A2M* and A2M*-mimicking Abs may occupy the A2M* binding site of LRP1, as already observed in other cells (4, 27). In cardiomyocytes, A2M* stimulated hypertonic cell growth by activating the extracellular signal-regulated kinase 1,2 and phosphoinositide 3-kinase/Akt pathway, a cellular effect that could be also detected by anti-LRP1 Ab. These findings corroborate our results, indicating that anti-LRP1 Abs mimic A2M* activities.

It remains obscure how A2M* and A2M*-mimicking Abs can stimulate cell proliferation in one cell type and inhibit proliferation and migration in others. Basically, one has to investigate whether these effects can be evoked by A2M*-associated growth factors or cytokines. This issue was addressed by Mantuano and colleagues (28), who convincingly reformulated that the receptor recognition sites of A2M alone can stimulate the Akt pathway. This accords with recent studies indicating that the endocytic and signaling events of LRP1 are functionally interconnected due to the affinity of certain motifs within the cytoplasmic receptor domain (e.g., NPXY and FXNPXY) to signal transduction adaptor protein (29).

A2M* was also reported to ligate signaling membrane receptors other than LRP1, such as the glucose-regulated protein 78 (Grp78). Targeting this receptor induced both cell proliferation and creation of an antiapoptotic milieu (30, 31). The different outcome with respect to cell proliferation and the fact that anti-LRP1 Abs mimic the action of A2M* may not approximate the conclusion that A2M* triggers Grp78 in astrocytoma cells.

A further pathway through which A2M is implicated is its capacity to inhibit and prime the clearance of proteases. Both A2M and LRP1 may affect the proteolytic potential at

plasma membrane and in the pericellular space by manipulating major elements of cell migration and invasion, e.g., MMP, plasmin, and plasminogen activators; all are direct ligands of LRP1 and can be endocytosed following complex formation with protease inhibitors. For instance, MMP-2 forms complexes with A2M (32) and conjugates to thrombospondin-2 as convincingly shown by Fears and colleagues (33). We used the activated A2M*, which has a locked conformation that is unable to bind and clear proteases. This excludes the antiproteolytic activity of A2M* as a possible mechanism.

The effect of LRP1 on tumor growth and invasiveness is well acknowledged (34); however, its precise role remains controversial. Inhibiting LRP1 expression and function is commonly reported to increase cell migration and invasion (11, 35–37). LRP1-deficient fibroblasts showed an increased cell migration (38), and restoration of LRP1 in LRP1-null cells markedly reduced cell growth, migration, and anchorage-independent colony formation and reduced tumor development in nude mice (39). Silencing of LRP1 by siRNA decreased cell migration (40) and prevented invasion of thyroid carcinoma cell lines despite increased pericellular proteolytic activity (34). The observed controversial results in response of cells to manipulations of LRP1 expression may depend on the specificity of cell environment, including interaction of LRP1 with other receptors or intracellular scaffold proteins. It becomes obvious that cellular effects induced by ligand-mediated inhibition of LRP1 are different from those created by silencing LRP1. It seems feasible that a genetically induced inactivation or deletion of LRP1 may disrupt its ability to control cell motility through interaction with other cell signaling receptors or membrane proteins (37). Therefore, it was our approach not to manipulate the phenotype of the tumor cells, e.g., by antisense or siRNA strategies, but rather to use specific natural agonists so as not to interfere with the potential role of LRP1 in regulating other possible functions.

Recently, the involvement of LRP1 in cell adhesion of human leukocyte as well as in cell-matrix interaction has been reported (41, 42). Hereby, we corroborate these reports by demonstrating the significant role of LRP1 and its ligand A2M* in tumor spheroid formation, cell adhesion, and cell-cell interaction.

In the present study, we offer a novel mechanism on how A2M*/LRP1 may regulate tumor cell growth, namely, by interfering with the Wnt/β-catenin signaling. Our findings coincide with results obtained by Guo and colleagues (43), who showed that blocking the Wnt/β-catenin signaling by indomethacin treatment caused β-catenin to relocate gradually from the cytoplasm and the nucleus to the plasma membrane. On the plasma membrane, β-catenin is known to form a complex with cadherins, maintaining adhesive junction and cell integrity (44). We propose a similar behavior in astrocytoma cells following exposition to A2M* as revealed by immunochemical studies. Therefore, the observed reduction of migration, invasion, and spheroid formation can be contributed to the induction of cellular cadherins, which act as tumor suppressors (44, 45). Moreover, consistent with our results is the up-regulation of FZD, which is found to decrease invasiveness and proliferation of thyroid carcinoma cells (46). In our opinion, the key event in A2M*-mediated attenuation of the Wnt/β-catenin signaling is the overexpression of LRP1. Zilberberg and colleagues (47) convincingly showed that FZD interacts with LRP1. Upregulation of the latter sequesters FZD, disrupts the FZD/LRP5/LRP6 complex, and ultimately represses the canonical Wnt pathway. Because MMPs and various oncogenes are downstream targets of Wnt/β-catenin signaling, the low expression level of LRP1, which was related to an aggressive and invasive phenotype of tumor cells, may therefore enable the canonical pathway (35, 48). Taken together, A2M* seems to exert its beneficial effect through the following: (*a*) upregulating LRP1 and FZD, (*b*) inhibiting expression of Wnt ligands and hence the autocrine activation of the Wnt/β-catenin signaling, and (*c*) the consequent relocation of β-catenin to the plasma membrane, which, together with upregulated cadherins, ameliorates cell integrity and thereby reduces cell proliferation, migration, and invasion potency. Therefore, it seems conceivable that modulation of Wnt/β-catenin pathway by A2M* may depend on the relative expression level of members of the LRP family, FZD, and secretory proteins, including Wnt ligands. How A2M* mediates this potential remains to be elucidated (Fig. 6).

Overall, the potential of A2M* to inhibit the malignancy-associated properties of human astrocytoma cells may warrant evaluating A2M* and anti-LRP1 for targeting Wnt ligands in gliobastoma and probably other tumors (49). In the light of these findings, we assume that the decline in the A2M blood level found at higher age may therefore facilitate tumor development (50).

Disclosure of Potential Conflicts of Interest

No potential conflicts of interest were disclosed.

Acknowledgments

We thank Dr. Mathias Platzer for the invaluable help, Angelika Schaefer and Elke Usbeck for their technical support, Dr. Dudley Strickland for his gift of the RAP-expressing plasmid, Dr. Anselm Berthold (Berthold Detection Systems, Pforzheim, Germany) for the kind disposal of an Orion II luminometer, Dr. Bruce J. Bryan (Prolume, Nanoligh, Inc., Pinetop, AZ) for the kind gift of *Gaussia* vector, and Dr. Sonya Faber for proofreading the text.

Grant Support

Wilhelm Sander-Stiftung grant 2006.053.2.

The costs of publication of this article were defrayed in part by the payment of page charges. This article must therefore be hereby marked *advertisement* in accordance with 18 U.S.C. Section 1734 solely to indicate this fact.

Received 4/21/09; revised 9/24/09; accepted 10/22/09; published online 1/4/10.

References

1. Newton CS, Loukinova E, Mikhailenko I, et al. Platelet-derived growth factor receptor-β (PDGFR-β) activation promotes its association with the low density lipoprotein receptor-related protein (LRP). Evidence for co-receptor function. J Biol Chem 2005;280: 27872–8.
2. McMahon B, Kwaan HC. The plasminogen activator system and cancer. Pathophysiol Haemost Thromb 2008;36:184–94.
3. Jodele S, Blavier L, Yoon JM, DeClerck YA. Modifying the soil to affect the seed: role of stromal-derived matrix metalloproteinases in cancer progression. Cancer Metastasis Rev 2006;25:35–43.
4. Padmasekar M, Nandigama R, Wartenberg M, Schluter KD, Sauer H. The acute phase protein α2-macroglobulin induces rat ventricular cardiomyocyte hypertrophy via ERK1,2 and PI3-kinase/Akt pathways. Cardiovasc Res 2007;75:118–28.
5. Arandjelovic S, Freed TA, Gonias SL. Growth factor-binding sequence in human α2-macroglobulin targets the receptor-binding site in transforming growth factor-β. Biochemistry 2003;42:6121–7.
6. LaMarre J, Wollenberg GK, Gonias SL, Hayes MA. Cytokine binding and clearance properties of proteinase-activated α2-macroglobulins. Lab Invest 1991;65:3–14.
7. Lillis AP, Van Duyn LB, Murphy-Ullrich JE, Strickland DK. LDL receptor-related protein 1: unique tissue-specific functions revealed by selective gene knockout studies. Physiol Rev 2008;88:887–918.
8. Paczek L, Gaciong Z, Bartlomiejczyk I, Sebekova K, Birkenmeier G, Heidland A. Protease administration decreases enhanced transforming growth factor-β1 content in isolated glomeruli of diabetic rats. Drugs Exp Clin Res 2001;27:141–9.
9. Lauer D, Muller R, Cott C, Otto A, Naumann M, Birkenmeier G. Modulation of growth factor binding properties of α2-macroglobulin by enzyme therapy. Cancer Chemother Pharmacol 2001;47 Suppl:S4–9.
10. Kirsch M, Schackert G, Black PM. Anti-angiogenic treatment strategies for malignant brain tumors. J Neurooncol 2000;50:149–63.
11. Song H, Li Y, Lee J, Schwartz AL, Bu G. Low-density lipoprotein receptor-related protein 1 promotes cancer cell migration and invasion by inducing the expression of matrix metalloproteinases 2 and 9. Cancer Res 2009;69:879–86.
12. Klaus A, Birchmeier W. Wnt signalling and its impact on development and cancer. Nat Rev Cancer 2008;8:387–98.
13. Birkenmeier G, Stigbrand T. Production of conformation-specific monoclonal antibodies against α2 macroglobulin and their use for quantitation of total and transformed α2 macroglobulin in human blood. J Immunol Methods 1993;162:59–67.
14. Baumgart Y, Otto A, Schafer A, et al. Characterization of novel monoclonal antibodies for prostate-specific antigen (PSA) with potency to recognize PSA bound to α2-macroglobulin. Clin Chem 2005;51:84–92.
15. Bradford MM. A rapid and sensitive method for the quantitation of microgram quantities of protein utilizing the principle of protein-dye binding. Anal Biochem 1976;72:248–54.
16. Birkenmeier G, Heidrich K, Glaser C, et al. Different expression of the α2-macroglobulin receptor/low-density lipoprotein receptor-related protein in human keratinocytes and fibroblasts. Arch Dermatol Res 1998;290:561–8.
17. Santel T, Pflug G, Hemdan NY, et al. Curcumin inhibits glyoxalase 1: a possible link to its anti-inflammatory and anti-tumor activity. PLoS ONE 2008;3:e3508.
18. Hollenbach M, Hintersdorf A, Huse K, et al. Ethyl pyruvate and ethyl lactate down-regulate the production of pro-inflammatory cytokines and modulate expression of immune receptors. Biochem Pharmacol 2008;76:631–44.
19. Hemdan NY. The role of interleukin-12 in the heavy metal-elicited immunomodulation: relevance of various evaluation methods. J Occup Med Toxicol 2008;3:25.
20. Pfaffl MW, Horgan GW, Dempfle L. Relative expression software tool (REST) for group-wise comparison and statistical analysis of relative expression results in real-time PCR. Nucleic Acids Res 2002;30:e36.
21. Chu CT, Pizzo SV. α2-Macroglobulin, complement, and biologic defense: antigens, growth factors, microbial proteases, and receptor ligation. Lab Invest 1994;71:792–812.
22. Sinnreich O, Kratzsch J, Reichenbach A, Glaser C, Huse K, Birkenmeier G. Plasma levels of transforming growth factor-1β and α2-macroglobulin before and after radical prostatectomy: association to clinicopathological parameters. Prostate 2004;61:201–8.
23. Williams SE, Ashcom JD, Argraves WS, Strickland DK. A novel mechanism for controlling the activity of α2-macroglobulin receptor/low density lipoprotein receptor-related protein. Multiple regulatory sites for 39-kDa receptor-associated protein. J Biol Chem 1992; 267:9035–40.
24. Pinner S, Sahai E. Imaging amoeboid cancer cell motility *in vivo*. J Microsc 2008;231:441–5.
25. Kunz-Schughart LA, Freyer JP, Hofstaedter F, Ebner R. The use of 3-D cultures for high-throughput screening: the multicellular spheroid model. J Biomol Screen 2004;9:273–85.
26. Wick W, Platten M, Weller M. Glioma cell invasion: regulation of metalloproteinase activity by TGF-β. J Neurooncol 2001;53:177–85.
27. Bacskai BJ, Xia MQ, Strickland DK, Rebeck GW, Hyman BT. The endocytic receptor protein LRP also mediates neuronal calcium signaling via *N*-methyl-D-aspartate receptors. Proc Natl Acad Sci U S A 2000;97:11551–6.
28. Mantuano E, Mukandala G, Li X, Campana WM, Gonias SL. Molecular dissection of the human α2-macroglobulin subunit reveals domains with antagonistic activities in cell signaling. J Biol Chem 2008;283:19904–11.
29. Stolt PC, Bock HH. Modulation of lipoprotein receptor functions by intracellular adaptor proteins. Cell Signal 2006;18:1560–71.
30. Misra UK, Sharma T, Pizzo SV. Ligation of cell surface-associated glucose-regulated protein 78 by receptor-recognized forms of α2-macroglobulin: activation of p21-activated protein kinase-2-dependent signaling in murine peritoneal macrophages. J Immunol 2005; 175:2525–33.
31. Misra UK, Deedwania R, Pizzo SV. Activation and cross-talk between Akt, NF-κB, and unfolded protein response signaling in 1-LN prostate cancer cells consequent to ligation of cell surface-associated GRP78. J Biol Chem 2006;281:13694–707.
32. Tchetverikov I, Verzijl N, Huizinga TW, TeKoppele JM, Hanemaaijer R, DeGroot J. Active MMPs captured by α 2 macroglobulin as a marker of disease activity in rheumatoid arthritis. Clin Exp Rheumatol 2003;21:711–8.
33. Fears CY, Grammer JR, Stewart JE, Jr., et al. Low-density lipoprotein receptor-related protein contributes to the antiangiogenic activity of thrombospondin-2 in a murine glioma model. Cancer Res 2005;65: 9338–46.
34. Dedieu S, Langlois B, Devy J, et al. LRP-1 silencing prevents malignant cell invasion despite increased pericellular proteolytic activities. Mol Cell Biol 2008;28:2980–95.
35. Desrosiers RR, Rivard ME, Grundy PE, Annabi B. Decrease in LDL receptor-related protein expression and function correlates with advanced stages of Wilms tumors. Pediatr Blood Cancer 2006; 46:40–9.
36. Nguyen DH, Webb DJ, Catling AD, et al. Urokinase-type plasminogen activator stimulates the Ras/extracellular signal-regulated kinase (ERK) signaling pathway and MCF-7 cell migration by a mechanism that requires focal adhesion kinase, Src, and Shc. Rapid dissociation of GRB2/Sps-Shc complex is associated with the transient phosphorylation of ERK in urokinase-treated cells. J Biol Chem 2000; 275:19382–8.
37. Webb DJ, Nguyen DH, Gonias SL. Extracellular signal-regulated kinase functions in the urokinase receptor-dependent pathway by which neutralization of low density lipoprotein receptor-related protein promotes fibrosarcoma cell migration and Matrigel invasion. J Cell Sci 2000;113:123–34.
38. Weaver AM, Hussaini IM, Mazar A, Henkin J, Gonias SL. Embryonic fibroblasts that are genetically deficient in low density lipoprotein receptor-related protein demonstrate increased activity of the urokinase receptor system and accelerated migration on vitronectin. J Biol Chem 1997;272:14372–9.

39. Zhang H, Lee JM, Wang Y, et al. Mutational analysis of the FXNPXY motif within LDL receptor-related protein 1 (LRP1) reveals the functional importance of the tyrosine residues in cell growth regulation and signal transduction. Biochem J 2008;409: 53–64.
40. Li Y, Lu W, Bu G. Essential role of the low density lipoprotein receptor-related protein in vascular smooth muscle cell migration. FEBS Lett 2003;555:346–50.
41. Gao R, Brigstock DR. Low density lipoprotein receptor-related protein (LRP) is a heparin-dependent adhesion receptor for connective tissue growth factor (CTGF) in rat activated hepatic stellate cells. Hepatol Res 2003;27:214–20.
42. Spijkers PP, da Costa Martins P, Westein E, Gahmberg CG, Zwaginga JJ, Lenting PJ. LDL-receptor-related protein regulates β2-integrin-mediated leukocyte adhesion. Blood 2005;105:170–7.
43. Guo Q, Wu M, Lian P, et al. Synergistic effect of indomethacin and NGX6 on proliferation and invasion by human colorectal cancer cells through modulation of the Wnt/β-catenin signaling pathway. Mol Cell Biochem 2009;330:71–81.
44. Bremnes RM, Veve R, Gabrielson E, et al. High-throughput tissue microarray analysis used to evaluate biology and prognostic significance of the E-cadherin pathway in non-small-cell lung cancer. J Clin Oncol 2002;20:2417–28.
45. Asano K, Duntsch CD, Zhou Q, et al. Correlation of N-cadherin expression in high grade gliomas with tissue invasion. J Neurooncol 2004;70:3–15.
46. Ulivieri A, Lavra L, Dominici R, et al. Frizzled-1 is down-regulated in follicular thyroid tumours and modulates growth and invasiveness. J Pathol 2008;215:87–96.
47. Zilberberg A, Yaniv A, Gazit A. The low density lipoprotein receptor-1, LRP1, interacts with the human frizzled-1 (HFz1) and down-regulates the canonical Wnt signaling pathway. J Biol Chem 2004; 279:17535–42.
48. Kancha RK, Stearns ME, Hussain MM. Decreased expression of the low density lipoprotein receptor-related protein/α 2-macroglobulin receptor in invasive cell clones derived from human prostate and breast tumor cells. Oncol Res 1994;6:365–72.
49. Hu J, Dong A, Fernandez-Ruiz V, et al. Blockade of Wnt signaling inhibits angiogenesis and tumor growth in hepatocellular carcinoma. Cancer Res 2009;69:6951–9.
50. Birkenmeier G, Muller R, Huse K, et al. Human α2-macroglobulin: genotype-phenotype relation. Exp Neurol 2003;184:153–61.